Experimental demonstration of hydraulic jump control in liquid metal channel flow using Lorentz force

A. E. Fisher, E. Kolemen, and M. G. Hvasta

Citation: Physics of Fluids **30**, 067104 (2018); doi: 10.1063/1.5026993
View online: https://doi.org/10.1063/1.5026993
View Table of Contents: http://aip.scitation.org/toc/phf/30/6
Published by the American Institute of Physics

Experimental demonstration of hydraulic jump control in liquid metal channel flow using Lorentz force

A. E. Fisher,[a] E. Kolemen, and M. G. Hvasta
Department of Mechanical and Aerospace Engineering, Princeton University, Princeton, New Jersey 08544, USA

(Received 26 February 2018; accepted 11 June 2018; published online 27 June 2018)

In this paper, hydraulic jump control using electromagnetic force in a liquid metal flow is presented. The control methods used give insight into the hydraulic jump behavior in the presence of magnetic fields and electrical currents. Flowing liquid metals is a proposed solution to heat flux challenges posed in fusion reactors, specifically the tokamak. Unfortunately, thin, fast-flowing liquid metal divertor concepts for fusion reactors are susceptible to hydraulic jumps that drastically reduce the liquid metal flow speed, leading to potential problems such as excessive evaporation, unsteady power removal, and possible plasma disruption. Highly electrically conductive flows within the magnetic fields do not exhibit traditional hydraulic jump behavior. There is very little research investigating the use of externally injected electrical currents and magnetic fields to control liquid metal hydraulic jumps. By using externally injected electrical currents and a magnetic field, a Lorentz force (also referred to as j × B force) may be generated to control the liquid metal jump behavior. In this work, a free-surface liquid metal—GaInSn eutectic or "galinstan"—flow through an electrically insulating rectangular duct was investigated. It was shown that applying a Lorentz force has a repeatable and predictable impact on the hydraulic jump, which can be used for liquid metal control within next-generation fusion reactors. *Published by AIP Publishing.* https://doi.org/10.1063/1.5026993

NOMENCLATURE

u	Flow velocity (m/s)
h	Flow depth (also referred to as height) (m), (cm), (mm)
0	Subscript for value upstream of a hydraulic jump (-)
1	Subscript for value downstream of a hydraulic jump (-)
g	Gravitational acceleration 9.81 (m/s^2)
Fr	Froude number upstream of the hydraulic jump (-)
Q	Volumetric flow rate (l/min)
F_L	Lorentz (j × B) force from externally injected electrical currents (N/m^3)
B	Magnetic field (T)
j	Electric current density (A/m^2)
I	Electric current (A)
w	Channel width 0.109 (m)
γ	Ratio of vertical j × B force to gravitational force (-)
ρ	Density of galinstan 6.4 × 10^3 (kg/m^3)
μ	Dynamic viscosity of galinstan 2.4 × 10^{-3} (Pa s)
S	Jump sensitivity (-)
ν	Kinematic viscosity of galinstan 3.75 × 10^{-7} (m^2/s)
σ	Electrical conductivity of galinstan 3.1 × 10^6 (S/m)
F_D	Drag force on liquid metal due to induced electrical currents (N/m^3)
L	Jump length (m)

[a]Author to whom correspondence should be addressed: aefisher@princeton.edu

I. INTRODUCTION

A. Background

Hydraulic jumps are well-known phenomena found in free-surface supercritical flows where thin, fast flow rapidly changes to thicker, slower flow. Hydraulic jumps have been studied for many applications, with the first study taking place nearly two hundred years ago.[1] The Froude number is the most important dimensionless parameter that is used to characterize hydraulic jump, and it is given in (1), with subscript 0 referring to conditions upstream of a jump,[2]

$$Fr = \frac{u_0}{\sqrt{gh_0}}. \tag{1}$$

A Froude number greater than unity implies that the flow is supercritical. This translates to the average flow velocity being greater than the wave speed, which enables a hydraulic jump to occur. There are several types and regimes of hydraulic jump, and the magnitude of the Froude number helps characterize the jump type.[3]

Mass and momentum conservation equations are used in order to derive some of the most useful equations for hydraulic jumps. For rectangular channels or ducts of constant width, (2) is used to express conservation of mass in an incompressible flow,[2]

$$Q = u_0 h_0 w = u_1 h_1 w. \tag{2}$$

Ignoring viscous losses and assuming constant duct width, (3) is used to express momentum conservation.[2] Neglecting viscous and other losses is a reasonable approximation as

the hydraulic jump takes place over a relatively short length, causing these losses to be small,

$$\frac{\rho g h_0^2}{2} + \rho u^2 h_0 = \frac{\rho g h_1^2}{2} + \rho u^2 h_1. \quad (3)$$

By manipulating (1)–(3), the depth change following a hydraulic jump can be derived, resulting in the classic relation given in (4),[2]

$$\frac{h_1}{h_0} = \frac{\sqrt{1+8Fr^2}-1}{2}. \quad (4)$$

Hydraulic jumps in traditional flows such as water coming out of a sluice gate have been thoroughly studied. However, hydraulic jumps in flows with added magnetohydrodynamic (MHD) effects are not as well understood. MHD effects result from highly electrically conductive fluids moving through magnetic fields and/or from externally injected electrical currents within the fluid interacting with the magnetic fields. The interaction between the externally injected electrical currents and the magnetic fields creates a Lorentz force (also referred to as a j × B force from the equation it is defined by). The force manifests as a body force on the flow given by (5). The electrical current density $\boldsymbol{j}$ here is given by (6),

$$\boldsymbol{F_L} = \boldsymbol{j} \times \boldsymbol{B}, \quad (5)$$

$$\boldsymbol{j} = \frac{\boldsymbol{I}}{wh}. \quad (6)$$

Here, $\boldsymbol{j}$ represents the electrical current flux vector, $\boldsymbol{B}$ is the magnetic field vector, $\boldsymbol{I}$ is the electrical current vector, w is the channel width, and h is the flow depth. This body force is somewhat analogous to gravity in the case of uniform electric current and magnetic field. A j × B force term may be added to (3), resulting in (7). This additional term has been used previously to predict flow depth changes in a channel due to j × B forces.[4] The chosen directional subscripts reflect the resultant equation based on the setup and convention of the presented experiments:

$$\frac{\rho g h_0^2}{2} + \frac{j_{0,x} B_z h_0^2}{2} + \rho u^2 h_0 = \frac{\rho g h_1^2}{2} + \frac{j_{1,x} B_z h_1^2}{2} + \rho u^2 h_1. \quad (7)$$

An equation similar in form to (4) may be derived by including the effects of the vertically directed Lorentz force in the momentum conservation equation. This yielded a new hydraulic jump equation shown in (8) and includes a substitution of a useful dimensionless number that relates j × B force to gravitational force,

$$\frac{h_1}{h_0} = \frac{-(1+\gamma_0) + \sqrt{(1+\gamma_0)^2 + 8Fr^2}}{2}. \quad (8)$$

The γ_0 term represents the ratio between the vertically (aligned with gravity) directed Lorentz force upstream of the jump and the gravitational force. A positive value of γ implies that the Lorentz force points in the same direction as gravity and can be evaluated at a location using (9), where the subscript $\hat{J}$ indicates the component aligned with gravity by chosen convention,

$$\gamma = \frac{(j \times B)_{\hat{j}}}{\rho g}. \quad (9)$$

B. Applications to nuclear fusion

Liquid metal plasma facing components (LM-PFCs) are of interest to a fusion reactor design due to their ability to actively remove large amounts of heat that solid-state components cannot handle.[5] Fast-flowing LM-PFC concepts rely on the liquid metal to remove heat from the plasma without getting so hot that the liquid metal excessively evaporates. These types of LM-PFC flows are projected to have thicknesses and flow speeds in the order of 0.5–2.0 (cm) and 10 (m/s), respectively.[6] These parameters in (4) predict a depth change factor of $\frac{h_1}{h_0} = 40$ following a hydraulic jump. Such a drastic change in flow depth would be catastrophic in application as the liquid metal would not drain properly, potentially flooding the reactor and causing rapid evaporation or disturbance to the plasma.

Of principal concern is whether a hydraulic jump is likely to occur in a thin, fast-flowing LM-PFC and how the addition of magnetic fields and externally injected electric currents may affect the onset of a jump. Thus, the position and depth change of the hydraulic jump in a liquid metal system were studied under various configurations to see how magnetic fields and the Lorentz force could be used to suppress, delay, or otherwise control hydraulic jumps.

The importance of having smooth, fast flow in a liquid metal divertor has been evaluated in the past, and the presence of hydraulic jumps is incompatible with this requirement.[7] Detailed studies have been done to evaluate evaporation in flowing liquid metals, and based on the expected temperature rise that would result from flow changes following a hydraulic jump, the evaporation would be far greater than allowable.[8]

C. Previous works

Free-surface liquid metal channel flows have received attention in past work in the context of fast-flowing LM-PFCs. Among the topics of interest, supercritical flow phenomena and hydraulic jumps have been studied.[9,10] Some research has also been done on hydraulic jumps taking place in highly electrically conductive flows within the magnetic fields.[11] However, work looking at the ways in which a hydraulic jump is affected by a Lorentz force created from externally injected electric currents and magnetic fields has not been thoroughly studied, and this is the main subject of the present paper.

Previous investigations performed by this research group quantified the effect of the Lorentz force generated through externally injected electrical currents and magnetic fields on the flow depth.[4] Upon inspection of momentum conservation equations, the depth changes were attributed to essentially increasing or decreasing "effective" gravity using the Lorentz force directed parallel or anti-parallel to gravity. This previous work did not investigate liquid metal hydraulic jumps.

II. EXPERIMENTAL OVERVIEW

The experimental results presented in this paper were obtained using the Liquid Metal eXperiment-Upgrade (LMX-U) test facility at the Princeton Plasma Physics Laboratory. Galinstan (GaInSn eutectic alloy) is used as the working

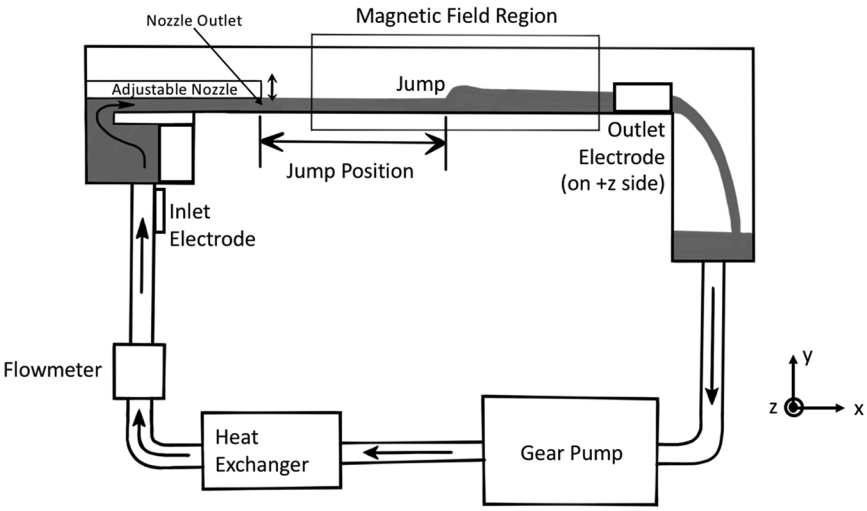

FIG. 1. The layout of the liquid metal loop—LMX-U. Not to scale.

liquid metal as it is liquid at room temperature and non-toxic. Several works on LMX have been recently published, which describe the system in more detail, with the upgraded components described in this work.[4,12]

A depiction of LMX-U can be found in Fig. 1. LMX-U used a 3HP rotary gear pump to circulate the liquid metal. A height-adjustable planar nozzle at the inlet allowed the inlet flow depth and speed to be changed for a given flow rate. Adjusting the height of the inlet nozzle led to a change in the channel flow depth, but for small nozzle heights this depth increased significantly further downstream of the nozzle. This effect is attributed to imperfections in the channel, leading to accumulated energy losses as well as channel wetting issues that caused the galinstan to thicken from the edges due to its large surface tension.

The pump and nozzle changes from the original LMX were intended to increase the flow rate and decrease the inlet depth, permitting the study of Froude numbers greater than unity. MHD drag was minimized by using acrylic channel walls to provide electrically insulating boundaries.[13]

Depth measurements were taken using a laser sheet incident on the surface of the liquid metal that is tracked by a CCD camera. This diagnostic has been used in past work on LMX as a non-intrusive height measurement.[4] The now upgraded sliding laser sheet configuration allows for measurements to be taken at various locations in the channel as both the laser sheet and the CCD camera slide with no relative motion. A depiction of the diagnostic is shown in Fig. 2, with a sample imaging of a hydraulic jump shown in Fig. 3. During testing, the laser sheet and the camera were manually swept over the jump.

Flow rates for each experiment were controlled using a variable frequency drive with a pump control resolution of 1 rpm. An Omega FMG96 electromagnetic flowmeter was installed downstream of the pump to verify the flow rate—the flowmeter was factory-certified to have less than 1% measurement error at the flow rates used in these experiments.

The magnet used for LMX-U is also described in past work and provides a magnetic field up to 0.33 (T) with roughly 4% field strength variation across the width of the test section.[4] A top-down view of the magnet setup is shown in Fig. 4 and a view along the channel in Fig. 5.

Electrodes located upstream of the channel inlet and near the outlet allowed for external electrical currents [140 (A)] to be injected into the flow using a DC power supply. The direction of the electrical current could be changed by swapping the polarity of the power supply. These electrode locations can be seen in Fig. 1.

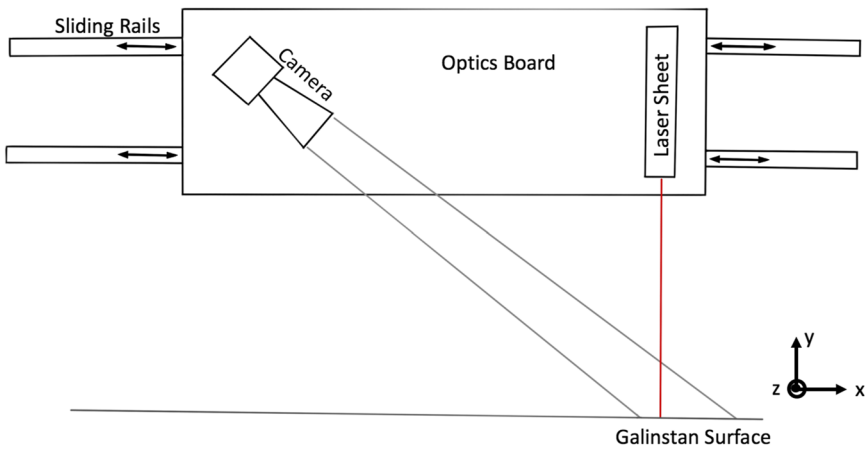

FIG. 2. Schematic of the sliding laser sheet setup.

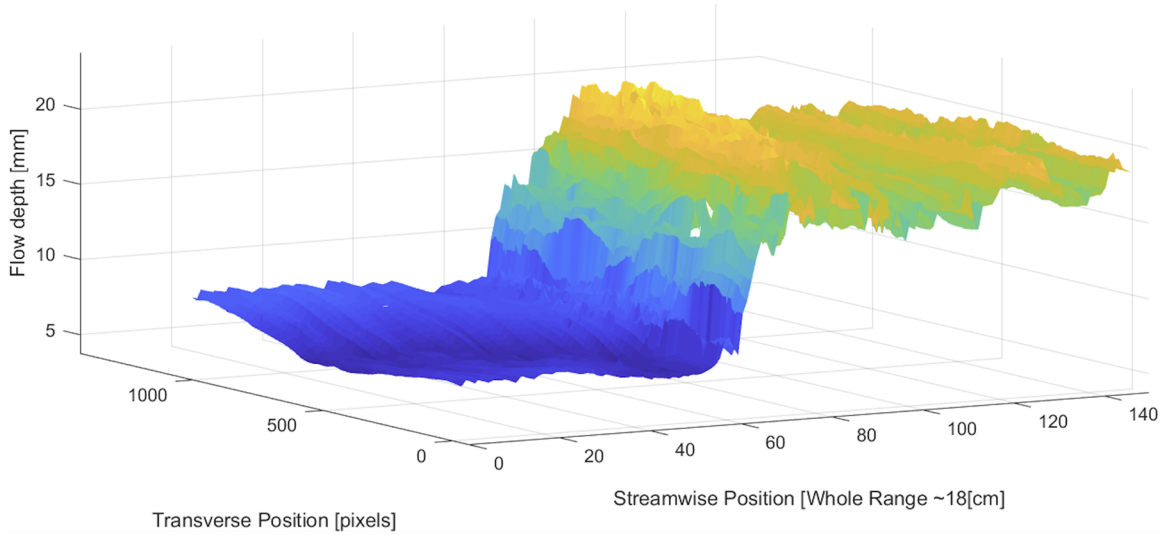

FIG. 3. Sample imaging of a hydraulic jump using laser sheet diagnostic.

To reach flows with the Froude number greater than one, either the flow rate was increased or the flow depth was decreased in accordance with (1). Decreasing flow depth also acted to increase the flow speed as the flow speed is inversely proportional to the depth according to (2), making flow depth the most impactful variable when trying to raise the Froude number.

It is important to note that over time, the galinstan oxidized even though LMX-U was purged of air with argon gas to avoid oxidization. The system may have had a small air leak, remnant air that could not be removed, or even oxygen impurities in the argon used to inert the channel. As the galinstan accumulated oxides, the flow characteristics eventually changed, requiring the oxides to be removed. Removal of oxides was done by allowing oxides to collect in the outlet waterfall on LMX-U as they are less dense than the galinstan and then unsealing the channel to scrape them off the top layer.

The data presented in each figure were collected during the same "cleaning" such that not enough oxides had accumulated to make significant changes to the flow behavior. Due to slight discrepancies in the cleanings, the system did not behave identically between cleanings, but this should not pose any major problems in analyzing the data. This effect made large data sets difficult to collect, resulting in the number of data points to be limited in a large parameter scan.

Galinstan has a large surface tension when compared with other liquids that are traditionally used in hydraulic jump experiments (nearly ten-times that of water), and it does not easily wet most conventional materials. The surface tension of galinstan was experimentally measured to be 0.61–0.62 (N/m) using a pendant drop experiment. Other sources have reported galinstan to have a surface tension of 0.533 (N/m); however, the amount of oxide on the galinstan surface is observed to change the surface tension and therefore cannot be determined exactly between cases as oxide levels varied.[14,15] The combination of these two effects causes non-negligible opposition forces to the liquid metal becoming too thin [minimum depth was roughly 6 (mm)]. Surface tension is also known to affect the hydraulic jumps; however, the effects were not thoroughly investigated in this study.[16]

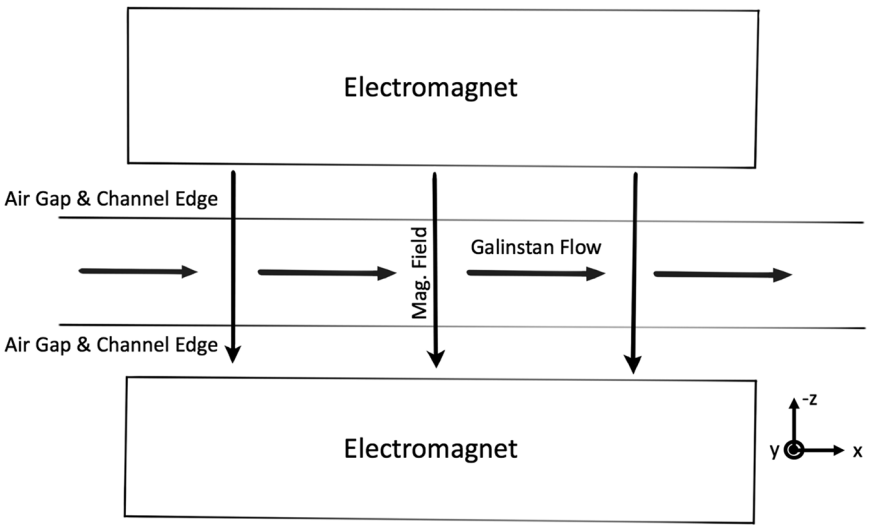

FIG. 4. An overhead depiction of the LMX-U electromagnet setup.

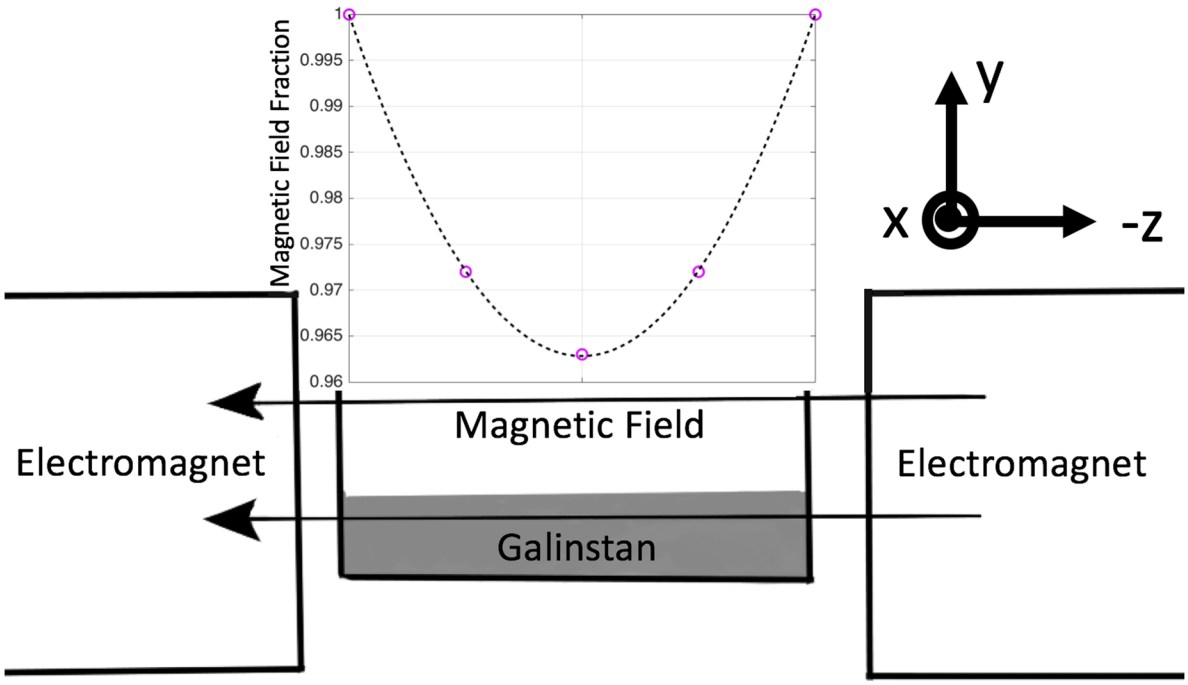

FIG. 5. The magnet strength across the channel width, looking down the length of the channel with flow out of the page.

III. HYDRAULIC JUMP CONTROL USING LORENTZ FORCE

A. Jump position

1. Flow rate dependence

Before using magnetic fields or electric currents, the jump position versus flow rate was measured as shown in Fig. 6. For this portion of the experiment, the nozzle height was kept at a constant 3 (mm). The flow range was limited from the ability to generate a jump at a minimum flow rate, as well as keeping the jump within the channel length.

The starting position of the jump was not determined from theory due to imperfections and non-wetting fluid behavior in LMX-U. A power-law curve fit of the data yielded a dependence on the flow rate with an exponent of 1.667, with less than 0.1% uncertainty in a 95% confidence interval. Expected behavior of jump position with flow rate may be seen in (10) and shows a dependence in complete agreement to the data.[17] The variable ν represents the kinematic viscosity of galinstan,

$$x_p \propto \left(\frac{Q}{w}\right)^{5/3} \nu^{-1} g^{-1/3}. \tag{10}$$

2. Magnetic field dependence

Jump location was measured for a variety of steady-state magnetic field strengths ranging from 0 to 0.15 (T) The nozzle height was kept fixed at 3 (mm) as it was in the jump position versus flow rate experiment, and flow rate was fixed at 22 (l/min). Even with the nozzle height at 3 (mm), the flow visibly increased in depth far upstream of the jump, leading to upstream jump depths greater than 8 (mm). Data for position as a function of magnetic field are shown in Fig. 7.

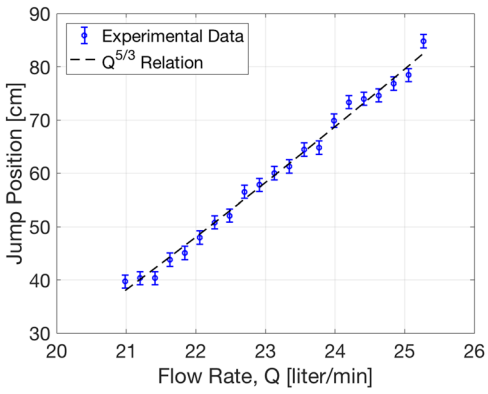

FIG. 6. Hydraulic jump location versus flow rate in channel. Jump position represents how far downstream from the nozzle outlet the jump occurred.

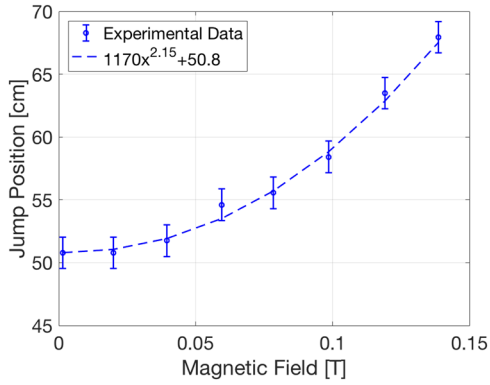

FIG. 7. Jump position versus magnetic field. Position is measured with respect to the nozzle outlet. Error bars represent 1.25 (cm) uncertainty in the jump position, assumed to be the full width at half maximum (FWHM).

The data points shown in Fig. 7 are fit using the form $y = ax^b + c$. A Monte Carlo curve fitting method was used to determine the range of possible power law fits considering measurement error. This analysis involved 10 000 curve fits on sets of normally perturbed data centered on each data point, with $\sigma = 0.531$. Position dependence on the magnetic field had a mean and standard deviation calculated, resulting in an exponent value of $b = 2.15 \pm 0.176$.

When increasing the magnetic field to 0.15 (T) and beyond, the hydraulic jump changed in nature and became less clear such that a position could not be determined. At high enough magnetic fields [approaching 0.3 (T)], the jump was suppressed entirely within the channel length and the flow remained supercritical up to the outlet.

A definitive relation explaining this curve was not determined. One explanation is a potential link to a reduction in "effective" viscosity caused by the magnetic field—thus causing the jump position to move downstream as suggested by (10). Past work on LMX shows a roughly $1/B$ dependence on "effective" viscosity as an explanation for the effect magnetic fields had on vortex shedding downstream of a cylinder.[18] This change in "effective" viscosity would predict a nearly linear dependence of jump position on magnetic field upon inspection of (10), namely, $x_p \propto \nu^{-1} \approx x_p \propto B^1$.

A second explanation is more generally attributed to how magnetic fields have effects on turbulent structures in conductive flows. The MHD drag appears as a body force in the momentum equation, given by (11). The variable σ is electrical conductivity of galinstan,

$$F_D = \sigma(\boldsymbol{u} \times \boldsymbol{B}) \times \boldsymbol{B}. \tag{11}$$

The ability of this force to restrict perturbations perpendicular to magnetic field has been shown to anisotropically reduce the flow turbulence.[19,20] The observed hydraulic jump position trend may be attributed to this force suppressing flow perturbations. However, other experiments have shown drag in the bulk flow direction to cause an upstream trend on jump position, opposite to the trends observed in this work—the differences can be mostly attributed to changes in experimental setup and magnetic field direction.[21] Because LMX-U has an electrically insulating duct, the bulk flow drag is reduced, but velocity perturbations are still damped.

3. j × B force dependence

Figure 8 shows a parameter scan of j × B force resulting from varying electrical current for three different magnetic fields. These three data sets were collected in the same channel cleaning to minimize differences in flow conditions between the different magnetic field settings.

The change in jump position was observed to exhibit similar behavior across the different magnetic field configurations. The slope of a linear fit varies by less than 2% between data sets. This consistency suggests that the j × B force effects are the same across different magnetic fields and there are no terms that depend on magnetic field alone. As such, the corresponding explanation from theory should reflect this. Based on previously mentioned work on LMX, j × B forces were found to change the flow depth. A known mechanism for a hydraulic jump to change position is due to changes in downstream depth, governed by the "sensitivity." Jump sensitivity is defined by[22]

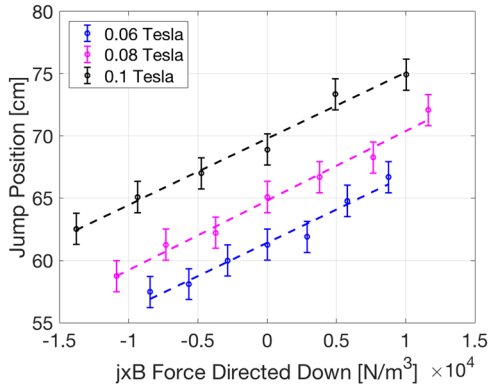

FIG. 8. Length-wise position of hydraulic jump versus j × B force directed downwards (i.e., a negative value implies the force is directed upwards against gravity). Position is measured with respect to the nozzle outlet. Magnetic field values represent a field fraction of 1 in Fig. 5.

$$S = \frac{\Delta x}{\Delta y}, \tag{12}$$

where Δx and Δy are changes in hydraulic jump location and flow depth downstream of the jump, respectively, as illustrated in Fig. 9.

One can also expect the nature of the jump to change due to the depth variation caused by the Lorentz force upstream of the jump, but decoupling the two effects is difficult.

As j × B force changed, the flow depth also changed. Compared with gravitational force, this is a relatively narrow regime of j × B force, and values of γ_0 stay below 0.25 in magnitude. Based on past results and measurements, the depth change in this regime is close to linear with respect to changes in j × B.[4] For the experimental case presented in Fig. 8, the depth change downstream of the jump over the j × B domain was measured to be $\Delta y = 0.9$ (mm), compared with the position shift of $\Delta x = 125$ (mm). A jump sensitivity of approximately 140 can then be calculated using (12). The theoretical sensitivity of the jump in LMX is plotted in Fig. 10, with the envelope resulting from changes in j × B force.

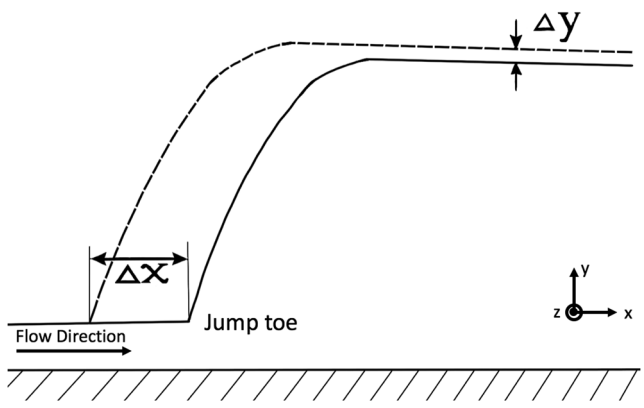

FIG. 9. A schematic showing Δx and Δy when calculating the sensitivity of a hydraulic jump—not to scale for jumps observed in LMX-U.

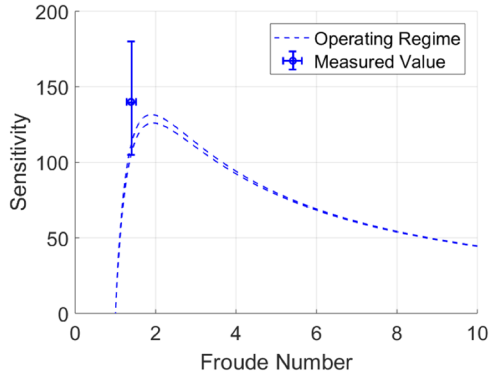

FIG. 10. Sensitivity calculated with Q = 22.3 (l/min), w = 0.109 (m), B = 0.1 (T), I = +135 (A) (upper bound), and I = −135 (lower bound). The Froude number is varied through changes in depth upstream of the jump. The error bar results from uncertainty in depth measurements needed to calculate S.

The curve is described by (19) and is derived in the general case using (8) rather than (4) in combination with (13) through (18).[22] For the presented case, the channel slope represented by the variable i is zero for LMX, leading to several terms dropping out in the final form of the equation.

For channels with small slopes, (13) relates the change in depth of the jump with downstream depth change. Due to the channel slope of LMX being zero, changes in jump depth are identical to downstream depth changes,

$$\Delta y = \Delta h_1 + i(\Delta x - \Delta L). \tag{13}$$

Taking the reciprocal of sensitivity with a substitution of (13) then results in (14),

$$\frac{1}{S} = \frac{\partial h_0}{\partial x}\left(\frac{\partial h_1}{\partial h_0} + i\left(\frac{\partial x}{\partial h_0} - \frac{\partial L}{\partial h_0}\right)\right). \tag{14}$$

The jump length given by L is approximated using (15) based on experimental results from the original author,

$$\frac{L}{h_0} = 9Fr - 9. \tag{15}$$

Differentiating (15) with respect to h_0 results in (16),

$$\frac{\partial L}{\partial h_0} = -4.5Fr - 9. \tag{16}$$

Differentiation on (8) results in (17),

$$\frac{\partial h_1}{\partial h_0} = \frac{2(1+\gamma) - 8Fr^2 - 2\sqrt{(\gamma+1)^2 + 8Fr^2}}{4\sqrt{(\gamma+1)^2 + 8Fr^2}}. \tag{17}$$

(18) shows the gradually varied flow equation in a rectangular channel,

$$\frac{\partial h_0}{\partial x} = \frac{i - j_f}{Fr^2 - 1}. \tag{18}$$

By combining (14) with (16)–(18) and performing some rearrangement, one can arrive at (19). This can be used to calculate an expected value of sensitivity,

$$S = \left(\frac{Fr^2 - 1}{j_f}\right)\left(\frac{2\sqrt{(\gamma_0+1)^2 + 8Fr^2}}{\sqrt{(\gamma_0+1)^2 + 8Fr^2} - (1+\gamma_0) + 4Fr^2}\right). \tag{19}$$

The variable j_f is a friction coefficient. This is solved numerically using a form of the Colebrook-White equation shown in (20) over a range of depths while holding the other variables constant; the Froude number increases as depth decreases according to (1),[23]

$$\frac{\left(\frac{Q}{w^{\frac{5}{2}}}\right)\sqrt{1 + \frac{2h_0}{w}}}{4\left(\frac{h_0}{w}\right)^{\frac{3}{2}}\sqrt{2gj_f}} = \log_{10}\left(\frac{3.187\sqrt{2gj_f}}{\left(1 + \frac{2h_0}{w}\right)^{\frac{3}{2}}}\left(\frac{h_0^{\frac{3}{2}}}{\frac{\mu}{\rho}}\right)\right). \tag{20}$$

The experimentally calculated sensitivity using (12) with measurements was subject to large experimental error but fell close to the predicted value from theory using (20). The Froude number varied from roughly 1.4 to 2 across experiments where sensitivity calculations remain relatively constant.

In general, sensitivity changes resulting from j × B force were relatively small and neglected, as shown in Fig. 10. For a larger range of j × B force, the change may need to be accounted for when trying to predict jump behavior.

B. Jump depth change

The depth ratio across the hydraulic jump was measured with changing j × B force. Measurements of h_0 were taken to be the depth leading up to the jump, while measurements

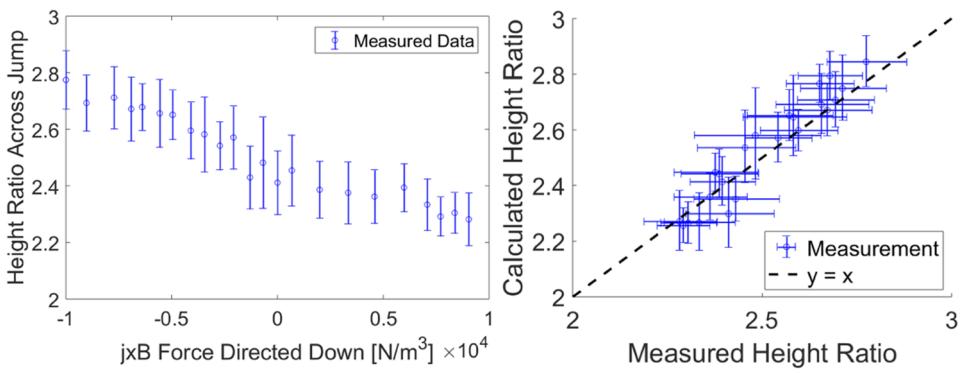

FIG. 11. Left: Data taken at various j × B forces. Right: Comparison between expected (calculated) ratio vs. measured. Error in calculated values results from the required h_0 measurement.

of h_1 were taken at the peak depth. For each flow condition, the sliding laser sheet was swept over the jump approximately ten times, each providing a depth measurement upstream and downstream of the jump. A 3 (mm) high weir was installed at the end of the channel during this experiment to measure the height ratio. This was done in order to more strictly enforce the subcritical condition at the end of the channel so that data could be taken at higher flow rates. The Froude number varied between 1.7 and 1.9 during these measurements as the upstream depth underwent small changes.

Measurements of h_1 were more variant than measurements of h_0 due to the turbulence created following the jump. Using (8), the expected h_1/h_0 value was calculated and compared with the measured value for various $j \times B$ forces. The trend of h_1/h_0 versus $j \times B$ and comparison between data and calculation are shown in Fig. 11. The data were taken while the system was operating at a flow rate of 28.7 (l/min), magnetic field of 0.082 (T), and electrical current varying from +/−140 (A).

Hydraulic jump depth ratio data are difficult to measure especially at these small scales, but the modified theory with the $j \times B$ force agrees well with the experimental observations and has a clear effect on the ratio.

IV. DISCUSSION

Hydraulic jumps pose a serious problem to fast-flowing liquid metal film PFCs by causing splashing and deceleration of flow that may lead to undesirable heating and evaporation. The results presented show how $j \times B$ force affects liquid metal hydraulic jumps and ways to prevent jumps from occurring.

The jump position change compared with $j \times B$ force for different magnetic field configurations is consistent, suggesting that the effects of $j \times B$ force are independent of the effects of a given magnetic field strength. As $j \times B$ force was increased to even higher values directed downwards not shown in the plots [greater than 1.5×10^4 (N/m^3)], the hydraulic jump changed in nature from a weak jump to an undular jump such that a jump position and depth ratio could not be taken and compared with results from the weak jump.

When using a magnetic field as high as 0.3 (T), there was no jump at all and the flow remained supercritical for the entire channel length. This is a positive result for liquid metals in a reactor setting as the transverse magnetic fields are 1–6 (T) which should provide a stronger jump suppression effect. It is difficult to make a direct comparison with reactor implementation though because some fast-flowing liquid metal divertor concepts may flow radially outwards, leading to circular hydraulic jumps that are different in nature.[24]

V. CONCLUSIONS AND FUTURE WORK

This experiment clearly demonstrated the control of a classical hydraulic jump using electromagnetic forces. Both the location and the depth ratio were shown to predictably vary with the use of magnetic fields and electrical currents.

Radial jump configurations were not investigated but may have more direct applicability to fusion reactors and are of great interest. In addition, the inclusion of a magnetic field gradient like that in a fusion reactor may produce new results. It is hoped that these experiments may be repeated in a reactor-relevant configuration with radial geometry and magnetic field gradients.

ACKNOWLEDGMENTS

The authors would like to thank K. Caspary, D. Dudt, E. Gilson, and Y. E. Yu for their assistance and insights throughout these experiments.

The research described in this paper was conducted under the Laboratory Directed Research and Development (LDRD) Program at Princeton Plasma Physics Laboratory, a national laboratory operated by Princeton University for the U.S. Department of Energy under Prime Contract No. DE-AC02-09CH11466.

This manuscript is based upon work supported by the U.S. Department of Energy, Office of Science, Office of Fusion Energy Sciences, and has been authored by Princeton University under Contract No. DE-AC02-09CH11466 with the U.S. Department of Energy. The publisher, by accepting the article for publication, acknowledges that the United States Government retains a non-exclusive, paid-up, irrevocable, worldwide license to publish or reproduce the published form of this manuscript, or allow others to do so, for United States Government purposes.

Digital data for this paper can be found at: http://arks.princeton.edu/ark:/88435/dsp01x920g025r.

[1] J. B. Bélanger, *Essai sur la Solution Numérique de Quelques Problémes Relatifs au Mouvement Permanent des Eaux Courantes* (Carilian-Goeury, Paris, 1828).
[2] V. T. Chow, *Open-Channel Hydraulics* (McGraw Hill Book Company, 1959).
[3] W. H. Hager, *Energy Dissipators and Hydraulic Jump* (Springer, Dordrecht, The Netherlands, 1992).
[4] M. G. Hvasta, E. Kolemen, A. Fisher, and H. Ji, "Demonstrating electromagnetic control of free-surface, liquid-metal flows relevent to fusion reactors," Nucl. Fusion **58**(1), 016022 (2018).
[5] M. A. Abdou, N. B. Morley, A. Y. Ying, S. Smolentsev, and P. Calderoni, "Overview of fusion blanket R&D in the US over the last decade," Nucl. Eng. Technol. **37**(5), 401–422 (2005).
[6] M. A. Abdou, "On the exploration of innovative concepts for fusion chamber technology," Fusion Eng. Des. **54**, 181–247 (2001).
[7] R. E. Nygren, T. D. Rognlien, T. D. Rensink, S. S. Smolentsev, M. Z. Youssef, M. E. Sawan, B. J. Merrill, C. Eberle, P. J. Fogarty, B. E. Nelson, D. K. Sze, and D. Majeski, "A fusion reactor design with a liquid first wall and divertor," Fusion Eng. Des. **72**(1-3), 181–221 (2004).
[8] R. W. Moir, "Liquid first walls for magnetic fusion energy configurations," Nucl. Fusion **37**(4), 557–566 (1997).
[9] N. B. Morley, *Numerical and Experimental Modeling of Liquid Metal Thin Film Flows in a Quasi-Coplanar Magnetic Field* (UCLA, Los Angeles, 1994).
[10] M. Narula, A. Ying, M. A. Abdou, and R. Moreau, "Liquid metal free surface flow through a non-uniform magnetic field: An experimental study," in Conference on Fundamental and Applied MHD, 2005.
[11] M. Narula, A. Ying, and M. A. Abdou, "A study of liquid metal film flow under fusion relevant magnetic fields," Fusion Sci. Technol. **47**, 564–568 (2005).
[12] M. G. Hvasta, E. Kolemen, and A. Fisher, "Application of IR imaging for free-surface velocity measurement in liquid-metal systems," Rev. Sci. Instrum. **88**, 013501 (2017).
[13] S. Malang and L. Buhler, *MHD Pressure Drop in Duct with Imperfectly Insulating Coatings* (Argonne National Laboratory, Lemont, IL, 1994).
[14] N. B. Morley and J. Burris, "The MTOR LM-MHD facility, and preliminary experimental investigation of thin layer, liquid metal flow in a 1/R toroidal magnetic field," Fusion Sci. Technol. **44**, 74–78 (2003).

[15]H. Ji, W. Fox, D. Pace, and H. L. Rappaport, "Study of small-amplitude magnetohydrodynamic surface waves on liquid metal," Phys. Plasmas **12**(1), 012102 (2005).
[16]R. I. Bowles and F. T. Smith, "The standing hydraulic jump: Theory, computations and comparisons with experiments," J. Fluid Mech. **242**, 145–168 (1992).
[17]J. K. Bhattacharjee and A. K. Ray, "Hydraulic jump," J. Phys.: Conf. Ser. **319**(1), 012003 (2011).
[18]J. R. Rhoads, E. M. Edlund, and H. Ji, "Effects of magnetic field on the turbulent wake of a cylinder in free-surface magnetohydrodynamic channel flow," J. Fluid Mech. **742**, 446–465 (2014).
[19]J. R. Rhoads, *Magnetohydrodynamics and Heat Transfer in a Free-Surface, Flowing Liquid Metal Experiment* (Princeton University, Princeton, 2013).
[20]A. Y. Ying, M. A. Abdou, N. Morley, T. Sketchley, R. Woolley, J. Burris, R. Kaita, P. Fogarty, H. Huang, X. Lao, and M. Narula, "Exploratory studies of flowing liquid metal divertor options for fusion-relevant magnetic fields in the MTOR facility," Fusion Eng. Des. **72**, 35–62 (2004).
[21]H. B. Löfgren and H. O. Åkerstedt, "Electromagnetic braking of the flow of a liquid metal with a free surface," Fluid Dyn. Res. **23**(1), 1–25 (1998).
[22]E. Wilson, "Location of the hydraulic jump in open rectangular channels," The Engineer **223**, 145–149 (1967).
[23]E. S. Crump, "Flow of fluids in conduits and open channels," Proc. Inst. Civ. Eng. **5**(4), 522–526 (1956).
[24]T. Bohr, C. Ellegaard, A. E. Hansen, and A. Haaning, "Hydraulic jumps, flow separation and wave breaking: An experimental study," Physica B: Condens. Matter **228**(1-2), 1–10 (1996).